

Chapter 6

Motor Imagery Experiment Using BCI: An Educational Technology Approach



**Camilo Andrés Ortiz Daza, Fredys A. Simanca H., Fabian Blanco Garrido,
and Daniel Burgos**

Abstract Three individuals participated in the experiment in a medical simulation lab at Bogotá's Antonio Nariño University. The objective was to compare the power spectral densities of signals obtained with a brain-computer interface (BCI) using a Nautilus g.tec 32, for activities that constitute motor imagination of closing the right and left hand, implementing a protocol designed by the author. The methodology used is closely connected to BCI-based HCIs with educational application. The results obtained indicate a clear intergroup difference in the levels of power spectrum, and a similarity in the intragroup levels. Measuring the signals of cognitive processes in the frontal and parietal cortex is recommended for educational applications. Among the conclusions, we highlight the importance of signal treatment, the differences encountered in spectrum comparison, and the applicability of the technology in education.

Keywords Brain-computer interface · Motor imagination · Digital filters · Power spectral density · Analysis of variance · Education

6.1 Introduction

The principal function of equipment called brain-computer interface (BCI) is measuring brain signals or central nervous system (CNS) activity in order to

C. A. Ortiz Daza
Clinical Foundation Shaio, Diagonal 115a # 70c 75, Bogotá, Colombia
e-mail: cortiz40@uan.edu.co

F. A. Simanca H. (✉) · F. Blanco Garrido
Free University of Colombia, Carrera 70 no. 53-40, Bogotá, Colombia
e-mail: fredysa.simancah@unilibre.edu.co

F. Blanco Garrido
e-mail: fabian.blancog@unilibre.edu.co

D. Burgos
Research Institute for Innovation & Technology in Education (UNIR iTED), Universidad
Internacional de La Rioja (UNIR), 26006 Logroño, La Rioja, Spain
e-mail: daniel.burgos@unir.net

restore, improve, complement, or obtain a natural outlet for the signal (McFarland & Wolpaw, 2017; Schalk, McFarland, Hinterberger, Birbaumer, & Wolpaw, 2004; Skola & Liarokapis, 2018). In turn, “*Brain signals can be acquired in a number of forms, including electrical (e.g., electroencephalography (EEG)) or magnetic fields (e.g., functional magnetic resonance imaging (fMRI)) or functional near infrared spectroscopy (fNIRS)*” (Daly & Huggins, 2015, p. 1). In rehabilitation applications, BCI translates incoming brain signals into outgoing signals; this is useful for the development of neuroprostheses (McFarland & Wolpaw, 2017; Skola & Liarokapis, 2018) to reactivate the body’s motor actions that have been lost due to severe conditions such as amyotrophic lateral sclerosis (ALS), strokes, and high-risk spinal cord injuries (McFarland & Wolpaw, 2017; Schalk, McFarland, Hinterberger, Birbaumer, & Wolpaw, 2004), through a process called motor imagery (MI). Figure 6.1 shows the structure of BCI for rehabilitation, which is modular and distributed into signal capture, its processing, and application.

The EEG signals are captured non-invasively through a cap or electrode array that captures the electric activity, as there is electrical contact resistance between the scalp and the electrodes. The tiny differences in potential or “evoked potential” are transmitted through the communication modules that send the encephalograph signals to a computer. A user interface or software digitally records the signal, processing it with the appropriate filters, by extracting the characteristics and the translation algorithm or “classifier”. Lastly, another communication system sends the information to the application designed for a particular type of rehabilitation. The following block diagram is for the BCI from Fig. 6.2, showing each of the stages from the capture of the signal to its arrival at the rehabilitation system.

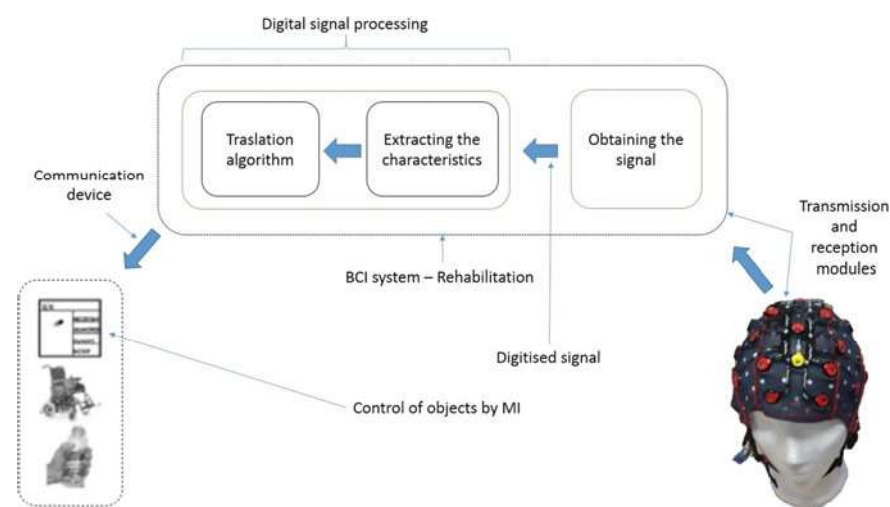


Fig. 6.1 BCI diagram. Prepared by the author, based on Schalk, McFarland, Hinterberger, Birbaumer and Wolpaw (2004)

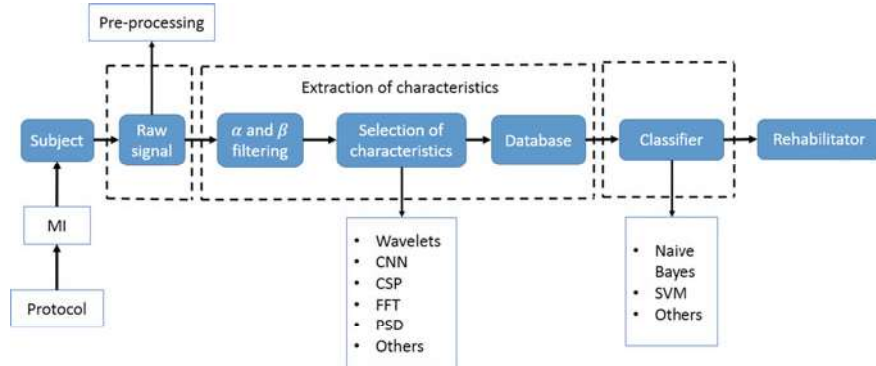


Fig. 6.2 Block diagram for rehabilitation BCI. Prepared by the author

Extracting the characteristics involves the identification of the relevant characteristics of the signals with motor imagination by separating the alpha and beta rhythms, since they contain the necessary components that lead to identifying said imagination (Bodda, et al., 2016; Chatterjee, Bandyopadhyay, & Sanyal Kumar, 2016; Shiratori, Tsubakida, Ishiyama, & Ono, 2015; Sun & Feng Ren, 2016). There are currently various methods for extracting the characteristics during the digital processing of EEG signals, including elliptical band-pass filters (Chatterjee, Bandyopadhyay, & Kumar Sanyal, 2016), finite impulse response (FIR) filters (Shiratori, Tsubakida, Ishiyama, & Ono, 2015), filter banks (Shiratori, Tsubakida, Ishiyama, & Ono, 2015), fast Fourier transform (FFT) (Chaudhary, Taran, & Bajaj, 2019), wavelet transform (WT) (Sun & Feng Ren, 2016; Xu, et al., 2018), wavelet coherence (WC) (Chaudhary, Taran, & Bajaj, 2019), round cosine transform (RCT), discrete cosine transform (DCT), multilayer perceptron (MLP) (Braga, Lopes, & Becker, 2018), and diffuse systems (Chaudhary, Taran, & Bajaj, 2019).

Diverse techniques may be used to classify signals with MI components, such as, among others, probability methods for time series (Chaudhary, Taran, Bajaj, & Sengur, 2019), fuzzy logic (Chaudhary, Taran, Bajaj, & Sengur, 2019; Das, Suresh, & Sundararaja, 2016), and neuron networks (Chaudhary, Taran, Bajaj, & Sengur, 2019; Zhu, et al., 2019) in order to identify patterns indicating that the signal has components of imaginary tasks. Similarly, common spatial pattern (CSP) (Chaudhary, Taran, & Bajaj, 2019; Jiao, et al., 2018; Xu, et al., 2018; Zhang, Yan, Hu, & Hong, 2017), support vector machine (SVM) (Xu, et al., 2018), Naïve Bayes method (Braga, Lopes, & Becker, 2018), convolutional neural networks (CNN) (Xu, et al., 2018), power spectral density (PSD) (Sun & Feng Ren, 2016), genetic algorithm (GA) (Jiao, et al., 2018), and independent component analysis (ICA) (Suarez Revelo, Ochoa Goméz, & Tobón Quintero, 2018a, 2018b), among others, are the most commonly used mechanisms for building the classifier algorithm, so the signals located at its output are the orders received by the neuroprosthesis in order to produce the imagined movement.

However, the inherent difficulty of identifying EEG signal patterns that correspond to motor imagination in the time domain as well as other domains (Chatterjee, Bandyopadhyay, & Sanyal Kumar, 2016; Sun & Feng Ren, 2016), and implementing the proper protocol for noting and obtaining these signals, constitutes a problem for developing the neuroprosthesis. In many cases, it is difficult to build a complete database of encephalograph signals due to the participant's fatigue and tiredness (Zhang, Yan, Hu, & Hong, 2017), since to develop MI “(...) the participants must learn to modulate their mental rhythms to have control, [which] is not an easy task (...)” (Skola & Liarokapis, 2018), therefore requiring a training phase to acquire the necessary skills.

Encephalograph signals must be modelled as time series, so they present phenomena such as shifts and random noise, which can be attributed to false contact between the electrodes and the scalp, blinking, jaw movement, or involuntary movement, among others (Kumar & Bhuvaneswari, 2012; Puthankattil Subha, Joseph, Rajendra Acharya, & Choo Min, 2010; Suarez Revelo, Ochoa Goméz, & Tobón Quintero, 2018a, 2018b); these are undesired and must be suppressed whenever possible.

Another BCI application significantly targets the education field, where systems called human-computer interface (HCI) have been developed to support learning deficiencies such as lack of attention and concentration (Serrhini & Dargham, 2017), flaws in motor or cognitive activities (Galway, Mc Chullagh, Lightbody, Brennan, & Trainor, 2015), and anxiety or psychological excitement presented by students, for example in mathematics education (Formunyuy & De Wet, 2015).

In that sense, the weaknesses presented lead to producing HCI that enables greater interaction with students and monitoring of their cognitive states—this means measuring the aforementioned flaws arising in elementary, primary, secondary, and university education. For these cases, the appropriate instrument is a BCI that configures feedback between the computerised system and the student, creating a closed-loop circuit. The measurement and interpretation of brain rhythms must indicate cognitive and psychological states in order to measure and predict the efficiency in the student's attention during the entire teaching-learning process (Katona & Kovari, 2018); however, the difficulty attributed to the MI process generates the same problem for BCI-based applications targeted at education.

In this case, the objective was to compare the PSDs of alpha and beta rhythms associated with imaginary tasks of closing the right and left hand, applying a protocol designed by the author to carry out the experiment. Each of the PSDs was analysed using one-factor analysis of variance (ANOVA), finding significant intergroup differences of PSD linked to MI and non-significant intragroup differences.

This led to the conclusion that the first participant obtained greater activity in the alpha rhythms related to the aforementioned MI tasks, while the third a predominance of beta rhythms for this type of activity. In the methods used, we highlight the model as a time series for the acquired signals, the filter design to extract alpha and beta rhythms, the Welch's method to calculate PSD, and the use of ANOVA to obtain the results of the experiment. The same methodology can be useful to identify potency levels associated with signals obtained in HCI with BCI employed in teaching-learning processes and especially in mathematics education.

6.2 Materials and Methods

6.2.1 Materials

The materials used to develop this chapter were the following:

- The Nautilus g.tec 32 BCI equipped with elements such as 32-electrode headset, two modules (one to transmit and one to receive), software called g.NEED access to measure electrode impedance, BCI2000 software that generates visual instructions, a Dell laptop, conductor gel for the electrodes, and other accessories.
- MATLAB R2018b software package to process and analyse the signals obtained.
- Fifty-inch LG television screen, used for the visual directions shown to each participant.
- Laboratory located at Antonio Nariño University in Bogota.

The methodology established to capture, process, and analyse each of the encephalograph signals for each participant is shown below.

6.2.2 Methodology

The methodology used for the experiment consisted of three stages, as follows.

6.2.2.1 Motor Imagination Practice

The protocol was followed for training each participant so that they naturally acquired motor imagination, carrying out the exercises in a closed, quiet, and comfortable setting. The exercises consist of closing the chosen hand (left or right) while the participant looks at it at all times. The sequence established is 10 unhurried, slow repetitions followed by an optional rest period of 10 s or more, repeating the process as many times as necessary. Afterwards, the participant must try to imagine the movements made as previously described with their eyes closed; this leads to verification that they have grasped the imagination. If not, the process must be repeated until they do.

6.2.2.2 Obtaining the Signal

Each of the BCI elements must be properly installed to ensure connectivity of the transmission and reception modules—the former is connected to the electrode headset while the latter must be connected to the laptop. Conductivity between the electrodes and the scalp is then verified by measuring impedance, which must not be greater than $30\text{ K}\Omega$ as they are active elements. The experiment begins, establishing

10 runs or sequences, each one consisting of 12 attempts called trials. During each trial, the participant has three seconds to imagine the indicated movement.

The experiment to obtain encephalograph signals had a running time of approximately one hour. The participants had been trained according to the established protocol. Each message presented during the course of the experiment was displayed on a television screen; the following figure illustrates the three visual instructions that they are given, i.e., “Wait to Start”, “Quiet”, “Relax”, MI, and “Time Out”. For the second-to-last visual aid, the participant is shown randomly placed arrows for the motor imagination process.

The Quiet stage lasts three seconds and indicates to the participant that they must not make any movement; Relax indicates that they should be relaxed and completely calm; MI prompts them to perform the task of imagining the movement of opening their hand towards the direction indicated by the arrow, left or right. In each instance, encephalograph signals are obtained, thus when the 10 runs are finished the experiment is over. Signals are not recorded during “Wait to Start” and “Time Out”, which tell the participant that the experiment is beginning and ending, and are not a part of the trial (Fig. 6.3).

The sequences composed of Quiet, Relax, and MI last nine seconds and are considered one trial. During the entire experiment with the three participants, a total of 360 MI signals were obtained, and 720 Quiet and Relax signals; they were analysed with MATLAB R2018b.

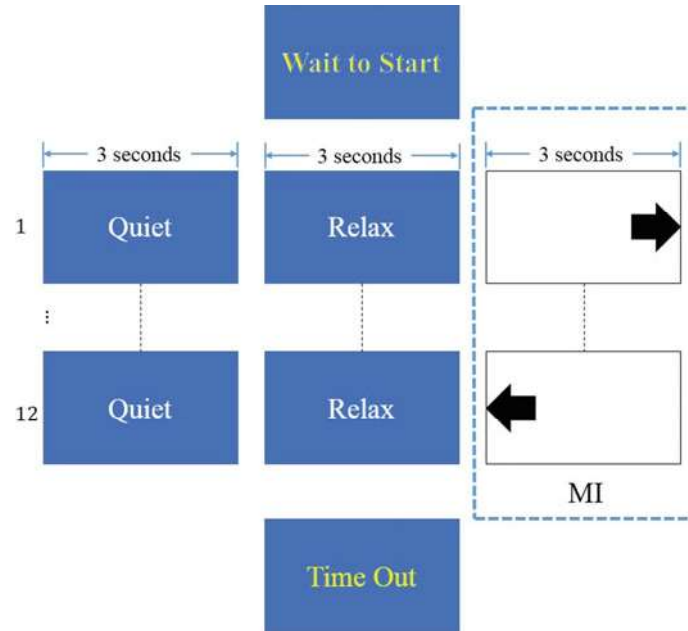


Fig. 6.3 Experiment stages for each participant. Prepared by the author

6.2.2.3 Digital Processing

This stage includes the following steps.

Signal Model as a Time Series

An encephalograph signal fluctuates unpredictably over time. It can be defined through a time series and is made up of shift, stationary, and random noise components; it is therefore feasible to represent it graphically before any analysis is made (Brockwell & Davis, 2002). Based on (Brockwell & Davis, 2002), a discrete time series may be written as:

$$X_n = m_n + S_n + Y_n \quad (6.1)$$

where X_n is a succession of samples in discrete time n , m_n is the shift component that is commonly deterministic, S_n is the stationary component, and Y_n is the random noise component; for EEG signals, the m_n and Y_n components can be attributed, for example, to eye blinking, jaw movement, and others. In general, the EEG signals obtained with BCI are mathematically represented as:

$$X_n = m_n + Y_n \quad (6.2)$$

X_n being the time series that represents each of the signals obtained. Commonly, the shift components can be written using the sum of discrete polynomials

$$m_n = \sum_{i=0}^k C_i n^i \quad (6.3)$$

where C_i represents the set of factors that accompany the time variable n , i is the polynomial grade formed by the shift component, and Σ is the abbreviated form to write the sum of polynomial terms. To eliminate m_n in (6.2), the differentiation method described in (Brockwell & Davis, 2002, p. 29) is used

$$\nabla^{k+1}(X_n) = \nabla^{k+1}\left(\sum_{i=0}^k C_i n^i\right) + \nabla^{k+1}(Y_k) \quad (6.4)$$

The ∇^{k+1} operator indicates the $k - n$ th difference plus the unit of each of the components that configure the time series of (6.2). Using the transformed unilateral Z (6.4), it is rewritten as:

$$\nabla^N(X_n) = C_n N! + \nabla^N(Y_n) \quad (6.5)$$

with $N = k + 1$. The repeated application of the ∇ operator eliminates the lineal, quadratic, cubic, or higher-level polynomial shift components, according to the case.

Pre-processing

The filter design in this stage is possibly the most important step for proper pre-processing, because one must bear in mind that the signals have shift and random noise components, referred to as artefacts. Artefacts are due to various factors such as eye blinking, facial movement, noise created by the electronic equipment, noise from the electrical power lines, and others. In some instances, electrocardiography (ECG), electromyography (EMG), and electrooculography (EOG) signals, among others, may also create artefacts, which are the most difficult to eliminate (Kaur & Kaur, 2015; Suarez Revelo, Ochoa Goméz, & Tobón Quntero, 2018a, 2018b).

Subsequently, the artefacts or random noise created while the signal is obtained should be mitigated while improving the signal-to-noise ratio (Raza, Rathee, Ming Zhou, Cecotti, & Prasad, 2019), making the signal pre-processing stage a priority for the classification of motor imagination signals (Parvinnia, Sabeti, Jahromi Zolghadri, & Boostani, 2014) enabling the selection of only relevant EEG signals (Soman & Murty, 2015). For this stage, a third-order high-pass filter was designed to eliminate very low frequency or cd artefacts, and a fifth-order notch filter was designed to mitigate 60 Hz frequency artefacts; both filters are Butterworth.

According to (Hossan & Mahmud Chowdhury, 2016), the American Electroencephalographic Society (AES) affirms that better signal resolution and transmission are obtained in the AF3, F7, F3, FC5, T7, P7, O1, O2, P8, T8, FC6, F4, F8, and AF4 electrodes, which are labelled according to the area where they are located—for example, the letter “F” corresponds to electrodes placed over the frontal region, “T” temporal, “C” central, “P” parietal, and “O” occipital. The letter “Z” indicates the middle area of the head (Kumar & Bhuvaneswari, 2012). However, in order to cover the entire motor cortex (Xia et al., 2017), using 13 electrodes is recommended: FC3, FCZ, FC4, C5, C3, C1, CZ, C2, C4, C6, CP3, CPZ, and CP4. Only electrodes C3 and C4 were considered for processing the signals obtained.

Rhythm Extraction

The literature indicates there are five signals that define an individual’s cerebral behaviour when performing any specific activity, and the following brain rhythms have been identified: delta “ δ ”, theta “ θ ”, alpha “ α ”, beta “ β ”, and gamma “ γ ”. This leads to five oscillators being defined for those rhythms according to their frequency range (Hu, Guo, & Liu, 2017; Suarez Revelo, Ochoa Goméz, & Tobón Quntero, 2018a, 2018b): 1–4 Hz for delta “ δ ”, 4–8 Hz for theta “ θ ”, 8–13 Hz for alpha “ α ”, 14–30 Hz for beta “ β ”, and 30–50 Hz for gamma “ γ ” (Hassan, Mahmoud, Abdalla, & Wedaa, 2015; Hossan & Mahmud Chowdhury, 2016; Hu, Guo, & Liu, 2017; Suarez Revelo, Ochoa Goméz, & Tobón Quntero, 2018a, 2018b).

To perform the observations corresponding to the imagination of closing the right and left hands, it was determined to only process the signals obtained on electrodes C3 and C4, due to their locations in the central region that dominate movement of the left and right hands, respectively (Chatterjee, Datta, & Kumar Sanyal, 2019). Similarly, it was decided to calculate the PSD of evoked potentials located in alpha and beta rhythms due to the high number of patterns of event-related desynchronisation (ERD) and event-related synchronisation (ERS). To that end, 8–13 Hz third-order and 14–30 Hz fourth-order elliptical pass band filters were used.

Power Spectral Density

To calculate the PSDs of the alpha and beta rhythms, the theoretical rationale used in research done by Rashid, Iqbal, Javed, Tiwana and Shahbat Khan (2018) and Puthankattil Subha, Joseph, Rajendra Acharya and Choo Min (2010) were utilised, applying the Welch's method that is recommended when there is scant signal data (Petre & Randolph, 2005). This power spectrum is described as:

$$S_{hh}(\Omega) = \frac{1}{F_s N U} |H_N(\Omega)|^2 \quad (6.6)$$

where F_s is the sample frequency, N the length or number of output signal samples from pass band filters $h[n]$, $H_N(\Omega)$ is the discrete-time Fourier transform (DTFT) of $h[n]$ and U the standardisation factor of the Hamming window, written as

$$U = \frac{1}{N} \sum_{n=0}^{N-1} |w[n]|^2 \quad (6.7)$$

The Hamming window used to calculate PSD in this paper was taken based on studies by Hassan, Mahmoud, Abdalla and Wedaa (2015), Oppenheim, Schafer and Buck (1999), Rashid, Iqbal, Javed, Tiwana and Shahbat Khan (2018) and Petre and Randolph (2005), defined as:

$$w[n] = 0.54 - 0.46 \cos\left(\frac{2\pi n}{N-1}\right) \quad (6.8)$$

The quantities attributed to each of the PSDs for the alpha and beta rhythms extracted from the database of the three participants, as well as the ANOVA, will be described in detail in the results section of this chapter.

6.3 Results

Results show the filter design for the digital processing of the EEG signals, the PSD estimation for alpha and beta rhythms with the Welch's method, and its comparison through a one-factor ANOVA.

6.3.1 Digital Processing

The pre-processing of the signal is integrated by two digital filters: one third-order high-pass filter and one fifth-order notch filter. Both were designed using bilinear transformation, taking into account the Butterworth approximation, and were implemented in MATLAB R2018b. The former has a band suppression frequency of 0.5 Hz, the latter has frequencies in the eliminated band from 58 Hz up to 62 Hz the mitigation assigned to both filters is 1 dB for the ripple and 60 dB for the suppression. Figure 6.4 illustrates, using DTFT, a magnitude and frequency graph for the first signal captured in the first participant, corresponding to Run 5, Trial 1, electrode C3, without filter (in black), and with pre-processing (in red).

It should be noted that due to pre-processing, the cd components were eliminated, and 60 Hz as well. An important aspect that was considered is signal lag; as the connection of high-pass filters followed by the notch filter presents negligible phase delay, implementing an all-pass section was unnecessary. However, if a 15-order low-pass filter was implemented with suppression frequency equivalent to the network, then said section would be required.

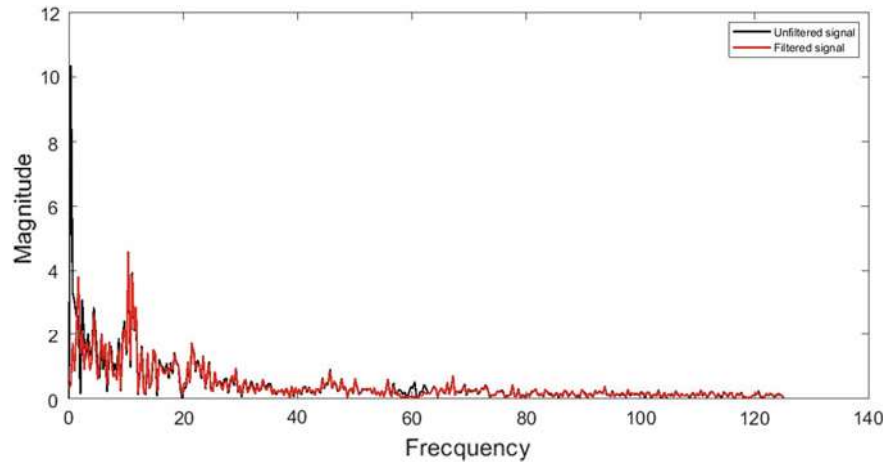


Fig. 6.4 Magnitude and frequency graph of stated EEG signal, without filter (in black) and processed (in red). Prepared by the author

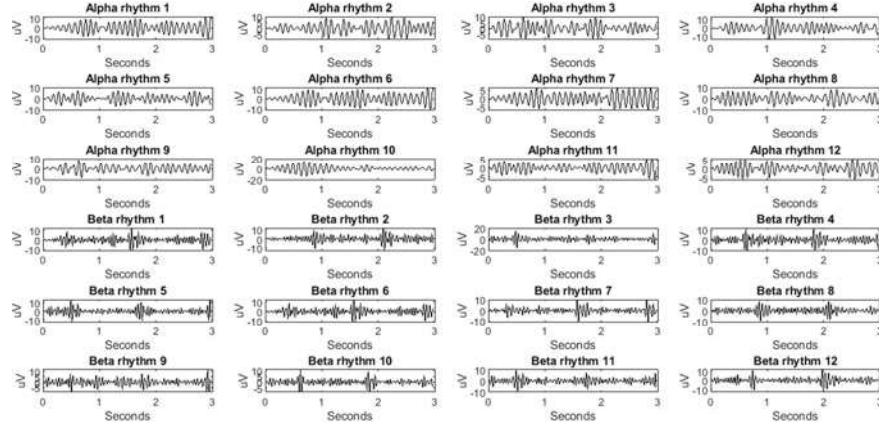


Fig. 6.5 Alpha and beta rhythms from Run 5, 12 trials, electrode C3, first participant. Prepared by the author

To extract alpha and beta rhythms, all frequencies greater than 60 Hz are considered noise and must be eliminated. Extracting said rhythms was achieved by implementing in MATLAB R2018b a third-order pass band filter with suppression frequencies of 8–13 Hz for alpha, and a 14–30 Hz fourth-order passband filter for beta. Both filters are elliptical, with pass ripple mitigation and 5 dB and 30 dB suppression, respectively. Figure 6.5 illustrates the alpha and beta rhythms associated with Run 5, in the 12 trials, for the first participant.

6.3.2 Power Spectral Density Calculation

The PSD calculation has been estimated using the aforementioned Welch's method, i.e., the (6.6), (6.7) and (6.8) equations were applied using FFT, calculated for each participant in Quiet, Relax, and MI states, taking the first, fifth, and last runs of the records obtained in the experiment.

In Fig. 6.6, the power spectra in black lines correspond to alpha rhythms divided in 18 for the left region and the same number for the right. The same occurs for the red lines which are PSDs for beta rhythms. These spectra were estimated for the MI state. Figures 6.7 and 6.8 illustrate the quantities calculated in $\text{dB}\mu\text{V}/\text{Hz}$ of the two rhythms in the abovementioned runs, and the PSDs plotted for the three participants in Quiet, Relax, and MI stages.

According to Fig. 6.7, the greatest amplitude recorded in the PSD calculations of the alpha rhythm in the MI stage is attributed to the first participant, with a value of $-0.7570 \text{ dB}\mu\text{V}/\text{Hz}$, followed by $-18.5637 \text{ dB}\mu\text{V}/\text{Hz}$ for the second, and -0.7570 , $-31.3264 \text{ dB}\mu\text{V}/\text{Hz}$ for the third. The lowest amplitudes are presented as follows: $-103.3667 \text{ dB}\mu\text{V}/\text{Hz}$ attributed to the last participant as recorded by C3 electrode in

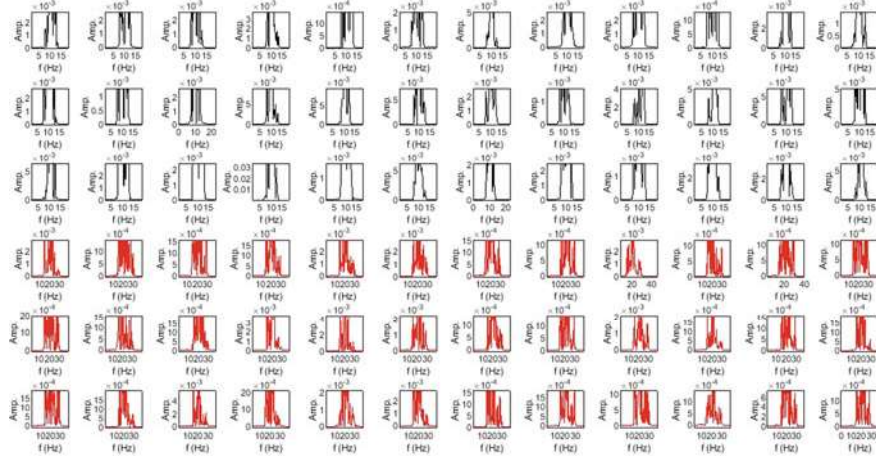


Fig. 6.6 PSDs of alpha and beta rhythms in Runs 1, 5, and 10 for the first participant. Prepared by the author

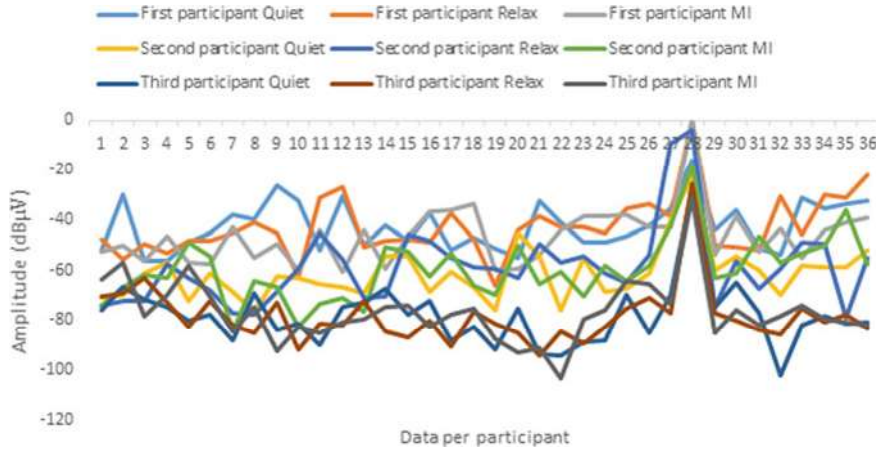


Fig. 6.7 Graph for PSD data of alpha rhythms. Prepared by the author

the fifth run and tenth trial, $-84.0527 \text{ dB}\mu\text{V/Hz}$ for the second participant as recorded by the C4 electrode in the first run and seventh trial, and $-60.3013 \text{ dB}\mu\text{V/Hz}$ for the first participant as taken from C4 in the last trial of the first run.

In the MI power spectrum calculations for beta rhythms as shown in Fig. 6.8, does not provide the same confidence like those mentioned for alpha rhythms were found. When comparing their densities, the greatest amplitude is attributed to the third participant with a PSD level of $-32.171 \text{ dB}\mu\text{V/Hz}$ in C3 in the last run, third trial, followed by $-44.9041 \text{ dB}\mu\text{V/Hz}$ attributed to the first participant in electrode C3 of the last run, and $-47.2197 \text{ dB}\mu\text{V/Hz}$ in the last run, sixth trial, electrode C3

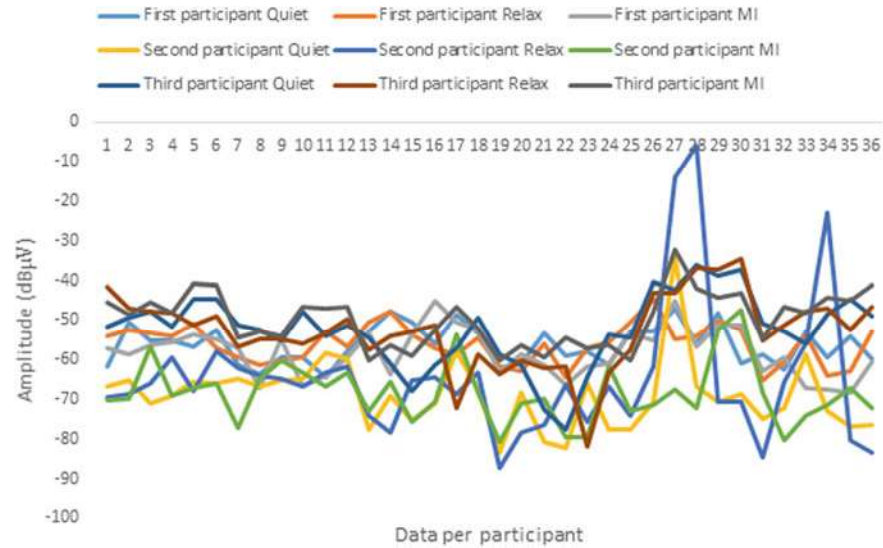


Fig. 6.8 Graph for PSD data of beta rhythms. Prepared by the author

for the second participant. Likewise, the lowest records are: $-80.6071 \text{ dB}\mu\text{V/Hz}$ for the second participant in the fifth run for electrode C4, $-68.1106 \text{ dB}\mu\text{V/Hz}$ for the first participant in the last run for electrode C4, and $-103.3667 \text{ dB}\mu\text{V/Hz}$ for the third participant in the fifth run, electrode C4.

6.3.3 Comparison of Power Spectra Using ANOVA

Before using one-factor ANOVA, we confirmed that the groups in the tables complied with the statistical assumptions of normality or normal distribution and uniformity of the variances, using the Kolmogorov-Smirnov test for the first case and Levene's test for the second. To begin with the proposed ANOVA, two hypotheses were established:

- H_0 or null hypothesis: rejected if the value of $p < 5\%$; for that to occur, the Fisher statistic $F \ggg p$. This hypothesis suggests that significant differences do not exist in each of the groups.
- H_1 or alternate hypothesis: accepted if $p < 5\%$, which means there are significant differences between the groups.

Upon analysing the intragroup data presented in Figs. 6.7 and 6.8, we chose as a dataset each stage of a trial as illustrated in Fig. 6.3, for each participant, obtaining the following results.

6.3.3.1 First Participant

The power spectra calculated for the alpha rhythms in Runs 1, 5, and 10, in states of Quiet, Relax, and MI, indicate that there are no significant differences between them given that $F(2.105) = 1.58$, $p < 5\%$, $\eta^2 = 0.029$. Likewise, the PSDs for the beta rhythms $F(2.105) = 1.74$, $p < 5\%$, $\eta^2 = 0.031$; for that reason, H_0 is accepted.

6.3.3.2 Second Participant

There are no significant differences in the power spectrum calculation for alpha and beta rhythms, given that $F(2.105) = 0.39$, $p < 5\%$, $\eta^2 = 0.0073$ and $F(2.105) = 1.33$, $p < 5\%$, $\eta^2 = 0.024$ respectively.

6.3.3.3 Third Participant

No significant differences are present in the PSDs of the alpha rhythms given that $F(2.105) = 0.24$, $p < 5\%$, $\eta^2 = 0.0044$, nor in beta due to $F(2.105) = 1.45$, $p < 5\%$, $\eta^2 = 0.026$. Therefore, the null hypothesis is accepted.

However, the intergroup analysis was done choosing only the data in the MI state (Fig. 6.3) for alpha and beta, forming a dataset of the three participants. The findings were as follows.

Comparing the power spectra of alpha rhythms in MI, we noted that significant differences exist given that $F(2.105) = 55.58$, $p < 5\%$, $\eta^2 = 0.51$. Using Bonferroni's method, we found that the associated means are -46.4791 , -59.8537 , and -76.6266 dB μ V/Hz from the first to the last participant, with an associated standard error of the method being 2.02.

The PSDs of the beta rhythms in the MI state evidence significant differences in the data groups. We obtained an $F(2.105) = 65.91$, $p < 5\%$, $\eta^2 = 0$, with means of -58.1451 , -68.3272 , and -49.7141 dB μ V/Hz for Participants 1, 2, and 3, respectively. The error found during this comparison was 1.148.

6.4 Recommendations

In education applications, BCI captures alpha and beta rhythms where the mechanisms described in Fig. 6.2 may be used. This allows the development of HCI to be applied in online education as indicated in Serrhini and Dargham (2017) or in computer games for mathematics education like those developed by Formunuy and De Wet (2015). The use of BCI supports the processes of educational feedback for affective computing, which in turn plays a very important role in education (Formunuy & De Wet, 2015). The stimuli can be visual, auditory, or optic, using

emerging technology such as augmented reality (AR) in the case of visual (Galway, Mc Chullagh, Lightbody, Brennan, & Trainor, 2015) or others.

However, capturing alpha and beta rhythms that indicate some state of inattention or psychological excitement is recommended, therefore measuring the evoked potentials must be undertaken in the frontal and parietal regions of the cerebral cortex (Serrhini & Dargham, 2017). Similarly, “(...) the frontal activity of the left side is associated with tendencies towards behaviour activating the motivational system, thus the activity on the right side is associated with tendencies towards general avoidance (...)” (Galway, Mc Chullagh, Lightbody, Brennan, & Trainor, 2015, p. 1555). This must be studied and considered for HCI applied to education.

6.5 Conclusion

The following conclusions are presented from the experiment, considering both the acquisition phase and digital processing.

A very important factor to keep in mind is the proper placement of the electrodes, as EEG signals can be affected by artefacts generated by constant blinking, poorly attached electrodes, poor placement, lack of training in motor imagination practice, and measuring of cognitive states, among others.

The time series model for encephalograph signals acquired with C3 and C4 electrodes enabled identifying and establishing the signal's shift components and random noise, which led to the choice of appropriate mechanisms for their digital processing.

Upon comparison and analysis of the power spectrum data, no significant differences were found between the datasets in states of Quiet, Relax, and MI, which make up each participant's experiment. However, selecting the PSD groups in the three participants' MI phases, we found notable differences, leading to the conclusion that the first participant obtained greater activity in the alpha rhythms corresponding to the MI state, with the third participant having the greatest predominance in the beta rhythms of motion imagination. In the majority of cases, the electrode that recorded the highest levels of PSD was the C3, with the C4 electrode acquiring the lowest levels.

The evolution of information technologies and artificial intelligence in education (AIED) must be researched in order to rapidly communicate and implement HCI, to provide permanent support to students through an affective computing system where aspects such as sensitivity and humanisation are key elements in the cognitive processes, as well as mitigating the flaws presented during the teaching-learning process. Therefore, the materials and methods used in the MI experiment can be applied to cognitive and psychological excitement processes, as in the case of mathematics anxiety.

References

- Bodda, S., Chandrapillai, H., Viswam, P., Krishna, S., Nair, B., & Diwakar, S. (2016). Categorizing imagined right and left motor imagery BCI tasks for low-cost robotic neuroprosthesis. In *International Conference on Electrical, Electronics, and Optimization Techniques (ICEEOT)* (pp. 3670–3673).
- Braga, R. B., Lopes, C., & Becker, T. (2018). Round cosine transform based feature extraction of motor imagery EEG signals. In *World Congress on Medical Physics and Biomedical Engineering* (pp. 511–515).
- Brockwell, P. J., & Davis, R. A. (2002). *Introduction to time series and forecasting*. New York: Springer.
- Chatterjee, R., Bandyopadhyay, T., & Sanyal Kumar, D. (2016). Effects of wavelets on quality of features in motor imagery EEG signal classification. In *2016 International Conference on Wireless Communications, Signal Processing and Networking (WiSPNET)* (pp. 1346–1350). Chennai, India: IEEE. <https://doi.org/10.1109/WiSPNET.2016.7566356>.
- Chatterjee, R., Datta, A., & Kumar Sanyal, D. (2019). Ensemble learning approach to motor imagery EEG signals classification. In N. Dey, A. S. Ashour, S. Borra, & F. Shi, *Machine learning in biosignal analysis and diagnostic imaging* (pp. 183–208). Elsevier Inc.
- Chaudhary, S., Taran, S., & Bajaj, V. (2019). Convolutional neural network based approach towards motor imagery tasks EEG signals classification. *IEEE Sensors Journal*, 1–7.
- Daly, J. J., & Huggins, J. E. (2015). Brain-computer interface: Current and emerging rehabilitation applications. *American Congress of Rehabilitation Medicine*, 96, 1–7.
- Das, A., Suresh, S., & Sundararaja, N. (2016). A discriminative subject specific spatio spectral filter selection approach for EEG based motor imagery task classification. In *Expert Systems with Applications* (pp. 375–384).
- Formunyuy, V., & De Wet, L. (2015). Using a brain computer interface (BCI) in reducing math anxiety: Evidence for South Africa. *Computers & Education*, 81, 113–122.
- Galway, L., Mc Chullagh, P., Lightbody, G., Brennan, C., & Trainor, D. (2015). The potential of the brain computer interface for learning: A technology review. In *2015 IEEE International Conference on Computer and Information Technology* (pp. 1554–1559). Liverpool, UK: IEEE.
- Hassan, M. A., Mahmoud, E., Abdalla, A. H., & Wedaa, A. (2015). A comparison between windowing FIR filters for extracting the EEG components. *Biosensors and Bioelectronics*, 1–7.
- Hossan, A., & Mahmud Chowdhury, A. M. (2016). Real time EEG based automatic brainwave regulation by music. In *5th International Conference on Informatics, Electronics and Vision (ICIEV)* (pp. 1–6). Dhaka, Bangladesh: IEEE. <https://doi.org/10.1109/ICIEV.2016.7760107>.
- Hu, H., Guo, S., & Liu, R. W. (2017). An adaptative singular spectrum analysis method for extracting brain rhythms of electroencephalographhye. *Peerj*, 1–17.
- Jiao, Y., Zhang, Y., Chen, X., Yin, E., Wang, X., & Cichocki, A. (2018). Sparse group representation model for motor imagery EEG classification. *IEEE Journal of Biomedical and Health Informatics*, 1–10.
- Katona, J., & Kovari, A. (2018). Examining the learning efficiency by a brain computer interface system. *Acta Polytechnica Hungarica*, 15, 251–280.
- Kaur, J., & Kaur, A. (2015). A review on analysis of EEG signals. In *International Conference on Advances in Computer Engineering and Applications ICACEA* (pp. 957–960).
- Kumar, J. S., & Bhuvaneswari, P. (2012). Analisys of electroencephalography (EEG) signals and its categorization: A study. *Procedia Engineering*, 38, 2525–2536. <https://doi.org/10.1016/j.proeng.2012.06.298>.
- McFland, D., & Wolpaw, J. R. (2017). EEG-based brain–computer interfaces. *Current Opinion in Biomedical Engineering*, 4, 194–200.
- Oppenheim, A. V., Schafer, R. W., & Buck, J. R. (1999). *Discrete time signal processing*. New Jersey: Prentice Hall.

- Parvinnia, E., Sabeti, M., Jahromi Zolghadri, M., & Boostani, R. (2014). Classification of EEG signals using adaptative weighted distance nearest neighbor algorithm. *Computing and Information Sciences*, 1–6.
- Petre, S., & Randolph, M. (2005). *Spectral analysis of signal*. New Jersey: Prentice Hall.
- Puthankattil Subha, D., Joseph, P. K., Rajendra Acharya, U., & Choo Min, L. (2010). EEG signal analysis: A survey. *Journal of Medical Systems*, 34, 195–212.
- Rashid, N., Iqbal, J., Javed, A., Tiwana, M. I., & Shahbat Khan, U. (2018). Design of embedded system for multivariate classification of fingers and thumb movements using EEG signals for control of upper limb prosthesis. *Hindawi BioMed Research International*, 1–11.
- Raza, H., Rathee, D., Ming Zhou, S., Cecotti, H., & Prasad, J. (2019). Covariate shift estimation based adaptative ensemble learning for handling non stationary in motor imagery related EEG based brain computer interface. *Neurocomputing*, 343, 154–166.
- Schalk, G., McFarland, D. J., Hinterberger, T., Birbaumer, N., & Wolpaw, J. R. (2004). BCI2000: A general-purpose brain-computer interface (BCI) system BCI2000: A general-purpose brain-computer interface (BCI) system. *Transactions on Biomedical Engineering*, 51, 1034–1044.
- Serrhini, M., & Dargham, A. (2017). Toward incorporating biosignals in online education case of assessing student attention with BCI. In A. Rocha, M. Serrhini, & C. Felgueiras (Eds.), *Europe and MENA cooperation advances in information and communication technologies* (pp. 135–146). Cham: Springer.
- Shiratori, T., Tsubakida, H., Ishiyama, A., & Ono, Y. (2015). Three-class classification of motor imagery EEG data including “Rest State” using filter bank multi-class common spatial pattern. In *The 3rd International Winter Conference on Brain Computer Interface* (pp. 1–4).
- Skola, F., & Liarokapis, F. (2018). Embodied VR environment facilitates motor imagery brain-computer interface training. *Computers and Graphics Journal*, 75, 59–71.
- Soman, S., & Murty, B. K. (2015). Using brain computer interface for synthesized speech communication for the physically disabled. *Procedia Computer Science*, 292–298.
- Suarez Revelo, J. X., Ochoa Gómez, J. F., & Tobón Quintero, C. A. (2018a). Validation of EEG pre-processing pipeline by test retest reliability. In *Applied computer sciences in engineering* (pp. 1–10).
- Suarez Revelo, J. X., Ochoa Goméz, J. F., & Tobón Quintero, C. A. (2018b). Validation of EEG pre-processing pipeline by test-retest reliability. In *Applied computer sciences in engineering. Communications in computer and information science* (Vol. 916, pp. 290–299). Cham: Springer. https://doi.org/10.1007/978-3-030-00353-1_26.
- Sun, L., & Feng Ren, Z. (2016). Classification of imagery motor EEG data with wavelet denoising and feature selection. In *International Conference on Wavelet Analysis and Pattern Recognition* (pp. 185–188). Jeju, South Korea: IEEE. <https://doi.org/10.1109/ICWAPR.2016.7731641>.
- Xia, B., Cao, L., Maysam, O., Li, J., Xie, H., Su, C., & Birbaumer, N. (2017). A binary motor imagery task based brain computer interface for two dimensional movement control. *Journal of Neural Engineering*, 1–8.
- Xu, B., Zhang, L., Song, A., Wu, C., Li, W., Zhang, D., ... Zeng, H. (2018). Wavelet transform time frequency image and convolutional network based motor imagery EEG classification. *IEEE Access*, 6084–6093.
- Zhang, R., Yan, Y., Hu, Y., & Hong, S. S. (2017). EEG function network analysis of left and right hand motor imagery. *National Nature Science Foundation of China*, 346–350.
- Zhu, X., Li, P., Li, C., Yao, D., Zhang, R., & Xu, P. (2019). Separated channel convolutional neural network to realize the training free motor imagery BCI systems. *Biomedical Signal Processing and Control*, 396–403.

Ortiz Daza Camilo Andres works as a biomedical engineer at the Shaio Clinical Foundation. His research lines are digital signal processing (DSP), electronic control and teaching—learning technologies in mathematical education, Specialist in electronic and biomedical instrumentation.

Fredys A. Simanca H. Systems Engineer, Universidad Cooperativa de Colombia, Bogotá, Colombia, researcher in the area of technologies in education, Research Professor, Ph.D. in Society of Knowledge and Action in the Fields of Education, Communication, Rights, and New Technologies.

Fabian Blanco Garrido Systems Engineer, Pilot University of Colombia, Bogotá, Colombia, researcher in the area of Telecommunications Networks, Research Professor at the Free University, Master in Telematics and Master in Computer Science Applied to Education.

Prof. Dr. Daniel Burgos works as a Full Professor of Technologies for Education & Communication and Vice-rector for International Research (UNIR Research, <http://research.unir.net>), at Universidad Internacional de La Rioja (UNIR, <http://www.unir.net>), a young 100% online university with over 40.000 students, 1.500 lecturers, 300 researchers, and premises in Spain, Colombia, México, Ecuador, Perú, Paraguay, Bolivia, Argentina and USA. In addition, he holds the UNESCO Chair on eLearning and the ICDE Chair in Open Educational Resources. He also works as Director of the Research Institute for Innovation & Technology in Education (UNIR iTED, <http://ited.unir.net>). Previously, he worked as Director of Education Sector and Head of eLearning & User Experience Lab in the Research & Innovation Department of the large enterprise Atos (<http://www.atos.net>), since 2007; and as assistant professor at the Open University of The Netherlands, before that (Welten Institute, <http://www.ou.nl/web/welten-institute/>). In 1996, he founded the first postgraduate online school on multimedia training and user interaction (ESAC), with over 6.000 students, worldwide.

His interests are mainly focused on Educational Technology & Innovation: Adaptive/Personalised and Informal eLearning, Open Science & Education, Learning Analytics, Social Networks, eGames, and eLearning Specifications. He has published over 140 scientific papers, 4 European patents, 14 authored books and 21 edited books or special issues on indexed journals. He is or has been involved in +55 European and Worldwide R&D projects, with a practical implementation approach.

In addition, he is a Professor at An-Najah National University (Palestine), an Adjunct Professor at Universidad Nacional de Colombia (UNAL, Colombia), a Visiting Professor at Coventry University (United Kingdom) and Universidad de las Fuerzas Armadas (ESPE, Ecuador). He has been chair (2016, 2018) and vice-chair (2015, 2017) of the international jury for the UNESCO King Hamad Bin Isa Al Khalifa Prize for the Use of ICTs in Education. He is a consultant for United Nations Economic Commission for Europe (UNECE), European Commission, European Parliament, Russian Academy of Science and ministries of Education in over a dozen countries. He is an IEEE Senior Member. He holds degrees in Communication (PhD), Computer Science (Dr. Ing), Education (PhD), Anthropology (PhD), Business Administration (DBA) and Artificial Intelligence (MIT, postgraduate).